

Algorithm for manoeuvres computation in Leader-Follower formation flights

Principal Author: J. Robles Agüera⁽¹⁾, Principal Author: J.A. Guio Justo⁽¹⁾,
Co-Author: A. Pérez González,⁽¹⁾ Co-Author: M. Sampietro Pou⁽¹⁾

⁽¹⁾ GMV Aerospace and Defence, SAU
Tres Cantos, Spain

Email: jrobles@gmv.com; juan.alberto.guio.justo@gmv.com;
adperez@gmv.com; msampietro@gmv.com

Abstract

In the space industry, the idea of coordinating multiple satellites to work together in formation has emerged as a new strategy. This approach is changing the way mission design is approached and executed. One of the key benefits of this approach is that it can enhance Earth observation performance, thereby improving our ability to observe and study the planet.

A new program has been developed to extend the functionality of GMV's *Focussuite* flight dynamics software to compute multiple formations, between reference and follower satellites. The development algorithm is able to inject a user satellite into formation with others and perform accurate station-keeping. The algorithm arranges the optimal precise manoeuvres required to achieve the relative target orbits and follow the leader by performing maintenance tasks. The algorithm also minimizes the total ΔV to conduct each operation.

I. INTRODUCTION

FAMA, *Formation Analysis and Manoeuvres Computation*, as part of the GMV Flight Dynamics product *Focussuite*, is the new program to support formation flying operations in Low Earth Orbits. Four different strategies can be achieved by the implemented algorithm: Pure Leader-Follower, Cartwheel, Pendulum, and Helix. The main purpose of the paper is to define the algorithms implemented to fulfil the acquisition and the maintenance of the formation.

A. Applications

This kind of the strategies potentially lies in Earth-Observation missions. In these kinds of missions, the formation of satellites allows to take the same image from different points at the same time, which will improve the accuracy of the reconstruction of the object. In future, formation flying usefulness will increase exponentially in several applications like topography, surveillance, and environmental monitoring.

The surveillance field will be enhanced also by formation strategies. The coordinated movement of several satellites will allow the expansion of the remote sensing coverage.

Additionally, the spacecraft inspection and maintenance tend to be for the formation field. The problem of debris in space is one of the major topics right now and there are a lot of missions to catch up with objects that are not useful anymore for deorbiting; or to increase their operative life by refuelling.

B. Types of formation

Four different strategies have been analysed and implemented as part of the *Focussuite* product.

Pure Leader-Follower: the more common strategy; one satellite is designated as the leader and the rest are the followers. The formation is defined by keeping constantly the same inter-satellite distance in the along-track direction. This has a direct effect on the argument of latitude (1). That means that in the pure leader-follower formation, the satellites will keep the same orbital parameters except for the argument of latitude, where there will be a delta depending on the distance that wants to be achieved.

Cartwheel: this strategy can be applied by adding a delta in the argument of perigee and the true anomaly which basically is going to rotate the eccentricity vector keeping the same module (3). With this change, the satellites are going to rotate inside the orbital plane one around the other.

Pendulum: in this case, the formation is obtained by changing the direction of the inclination vector. In this case, as the difference is in the out-of-plane direction (3), this formation is more difficult to maintain.

Helix: if the last two formations are applied at the same time, Helix is the resulting strategy. In this formation, both the eccentricity and inclination vector of the different satellites are rotated keeping the same modulus (4). As a result, one of the satellites is making a helix around the leader one.

II. ALGORITHM DEVELOPMENT

We present here the core functionality algorithm, a program featured in GMV's software product *Focussuite*, called FAMA, *Formation Analysis and Manoeuvres computation*.

A. Formation target definition

The target orbit is based on the leader satellite orbit, aligned with the user-specified formation parameters, which oversees defining a perfect formation between the leader and follower (reference and user satellite). The orbital osculating elements set to use along the paper will be $x(t) = (a, e, i, \Omega, \omega, \theta)$.

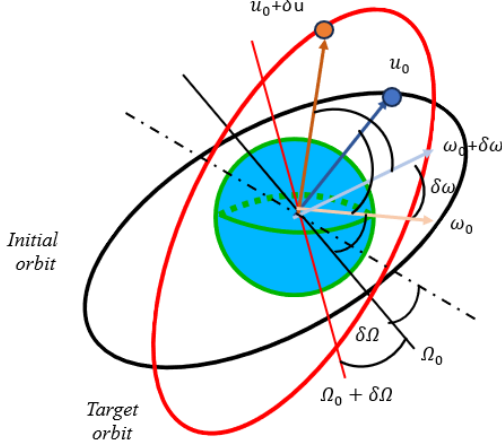


Fig. 1. Orbital target orbit definition calculated from Leader satellite.

Argument of latitude is used instead ($u = \omega + \theta$) to make it more convenient for near-circular orbits. The target orbit will be based on the classic mean orbital element. To compute the mean elements, multiple theories are available [2]. One of the most common forms and the one used is the direct average along one orbit for every point in the arc to compute (1).

$$\bar{x}_n(t_n) = \frac{1}{2\pi} \int_{u_n - \pi}^{u_n + \pi} x(t) du \quad (1)$$

To define the formation target orbit, the orbital elements will be the same as the Leader orbit $\bar{x}_t(t) = \bar{x}_l(t)$ along the time in the first instance. Depending on the selected formation, the target acquires multiple configurations according to user selection (2-5). δu , $\delta \omega$, $\delta \theta$ and $\delta \Omega$ are the user input parameters which define each formation type, Fig 1. For every time step, the delta variation is defined as constant in mean elements.

$$\text{Leader Follower } \bar{u}_t(t) = \bar{u}_l(t) + \delta u \quad (2)$$

$$\text{Cartwheel} : \begin{cases} u_t(t) = \bar{u}_l(t) + \delta u \\ \omega_t(t) = \bar{\omega}_l(t) + \delta \omega \end{cases} \quad (3)$$

$$\text{Pendulum} : \begin{cases} u_t(t) = \bar{u}_l(t) + \delta u \\ \Omega_t(t) = \bar{\Omega}_l(t) + \delta \Omega \end{cases} \quad (4)$$

$$\text{Helix} \begin{cases} \bar{\omega}_t(t) = \bar{\omega}_l(t) + \delta \omega \\ u_t(t) = \bar{u}_l(t) + \delta u \\ \bar{\Omega}_t(t) = \bar{\Omega}_l(t) + \delta \Omega \end{cases} \quad (5)$$

In the case of a simple leader-follower formation, the user could want to define the inter-satellite distance instead of orbital parameter differences (2). If the selected distance r is much smaller than the semi-major axis ($\delta r \ll a$), the Δu to shape the formation could be expressed as (6).

$$\Delta u = 2 a \sin\left(\frac{\delta r}{a}\right) \quad (6)$$

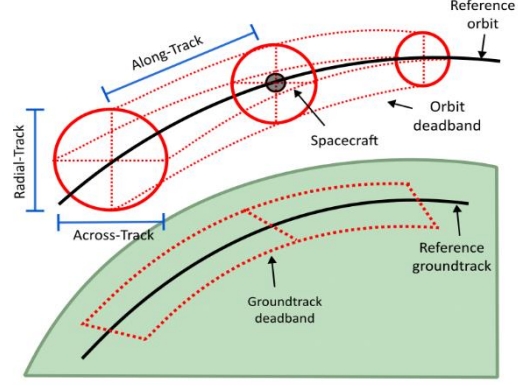


Fig. 2. Orbital tube threshold defined over formation target orbit.

Threshold definition on the target orbit

To maintain the orbit inside a correct threshold formation, an orbital “tube” around the computed target must be defined, Fig. 2.

The threshold typically will be defined in relative cartesian elements. Considering a Radial-Transversal-Normal (RTN) system from target satellite orbit. The Cartesian Hill frame coordinates are used in the following development. Defining semi-latus rectum parameter $p = a(1 - e^2)$, and mean motion $n^2 = \mu/a^3$, the relative position vector components in smaller distances are given in terms of orbit element differences from the target orbit through [3] (7):

$$\begin{aligned} \Delta x &\approx \frac{r}{a} \Delta a + \frac{V_r}{V_t} r \Delta \theta - \frac{r}{p} (2ae_x + r \cos \theta) \Delta e_x \\ &\quad - \frac{r}{p} (2ae_y + r \sin \theta) \Delta e_y \\ \Delta y &\approx r (\Delta \theta + \cos(i) \Delta \Omega) \\ \Delta z &\approx r (\sin(\theta) \Delta i - \cos(\theta) \sin(i) \Delta \Omega) \end{aligned} \quad (7)$$

The radial and transverse velocity components V_r and V_t respect to target position is defined as (8).

$$\begin{aligned} V_r &= \dot{r} = \frac{h}{p} (e_x \sin \theta - e_y \cos \theta) \\ V_t &= r \dot{\theta} = \frac{h}{p} (1 + e_x \cos \theta + e_y \sin \theta) \end{aligned} \quad (8)$$

Where equinoctial eccentricity elements are used for simplicity in this case $e_x = e \cos \omega$, $e_y = e \sin \omega$.

B. Formation target acquisition

After calculating the target orbit, our next step involves verifying whether the follower satellite is within the boundaries of the calculated trajectory. The most cases, the initial satellite position will be located outside the selected threshold.

Therefore, the relocation injection algorithm starts to compute the multi-manoeuvre path. This step is the most complex, due to formation requires high precision in target acquisition. In addition, a minor amount of the total ΔV , to reduce to minimum mass consumption will be searched. Besides, the new modern LEO typically use low thrust propulsion, which implies an incredibly low ΔV per manoeuvre, so a multiple manoeuvre path will be performed in the process. The strategy proposed to fulfil the previous condition will consist of a set of successive manoeuvres to correct directly a, e, i and ω , but taking advantage of a drifting intermediate, well known as coasting orbit, to correct naturally Ω and u , Fig. 3.

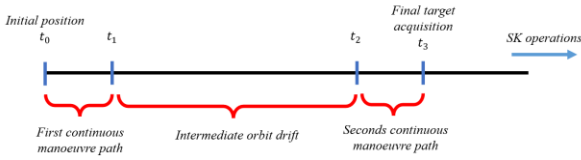


Fig. 3. Relocation steps in timeline schema.

Coasting orbit drifting path

The principal perturbations impacting satellites in LEO orbits are Earth's oblateness, atmospheric drag, and solar radiation pressure. The direct satellite movement due to gravitational law, and the most important perturbation, Earth's oblateness, affects the secular movement of Ω , ω , and M through the parameter J_2 [1], so it is possible to get the drifting value respect from time (9)

$$\begin{aligned} \dot{\Omega}_{sec} &= -\frac{3J_2 R_{\oplus}^2 n \cos(i)}{2p^2} \\ \dot{u}_{sec} &= n + \frac{3nJ_2 R_{\oplus}^2 (4 - 5 \sin^2 i)}{4p^2} - \frac{3nR_{\oplus}^2 J_2 \sqrt{1-e^2} (2 - 3 \sin^2 i)}{4p^2} \end{aligned} \quad (9)$$

Considering setting a drifting intermediate orbit respected from the target, it is possible by taking increments from them, i.e. $\Delta \dot{\Omega}_{int} = \dot{\Omega}_{int} - \dot{\Omega}_t$ and $\Delta \dot{u}_{int} = \dot{u}_{int} - \dot{u}_t$. For low eccentricity orbit, and neglecting other important effects, it is possible to take increments over the previous equation (10).

$$\begin{aligned} \Delta \dot{\Omega}_{int} &\approx f_{\Omega}(\Delta i_{int}) + f_{\Omega}(\Delta a_{int}) \\ \Delta \dot{u}_{int} &\approx f_u(\Delta a_{int}) \end{aligned} \quad (10)$$

The expression proves that an incremental value from the target orbit induces a drift in Ω , and u . Establishing a precise Δa_{int} over the desired target orbit, the user satellite started u position drift to the final one naturally, without any manoeuvres during this period. A positive Δa_{int} generates a negative drift $\Delta \dot{u}_{int}$ drift, Fig. 4. Instead, a positive Δa_{int} and positive Δi_{int} as well, as generate a negative $\Delta \dot{\Omega}_{int}$, Fig. 5, and vice versa.

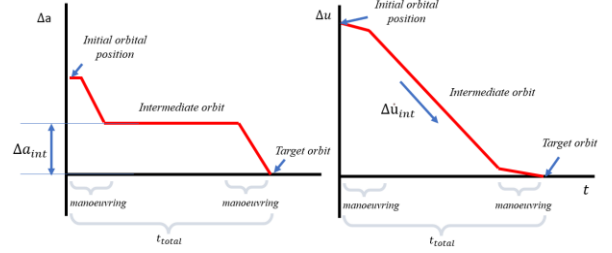


Fig. 4. Drifting Δu user satellite by an induced Δa_{int} over target orbit.

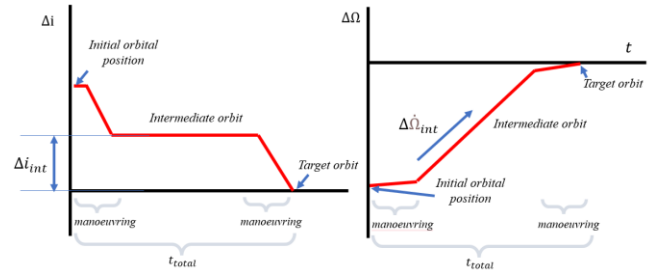


Fig. 5. Drifting $\Delta \Omega$ user satellite by an induced Δi_{int} over target orbit.

The incremental value will be suited according to the user's total available time to perform the relocation. Measuring the total $u_{ini} - u_t$ to correctly relocate the user satellite, according to the total available time for formation acquisition relocation t_{total} , the $\Delta \dot{u}_{int}$ can be suited as (11).

$$f_u(\Delta a_{int}) \approx -\frac{u_{ini} - u_t}{t_{total} - \frac{t_{man}}{2}} \quad (11)$$

The total number of orbit period manoeuvring times is not calculated yet but could be solved interactively as will be proposed later.

Typically, Ω is a highly costly relocation parameter. To solve this problem, a similar approach as argument of latitude. In the incremental equation, $\Delta \dot{\Omega}_{int}$ has an equal dependence of Δi and Δa . Due to the Δa_{int} is imposed by u drifting, Δi_{int} from target orbit should be suited directly by excluding $f_{\Omega}(\Delta a_{int})$ [4]. Therefore, the total

$\Delta\dot{\Omega}_{int}$ in a first iteration could approximately by (12).

$$f_{\Omega}(\Delta i_{int}) \approx -\frac{\Omega_{ini}-\Omega_t}{t_{total}-\frac{t_{man}}{2}} - f_{\Omega}(\Delta a_{int}) \quad (12)$$

For later calculus, as though the total relocation time is imposed, $f_{\Omega}(\Delta i_{int})$ and $f_u(\Delta a_{int})$ behave like unknown variables, which are imposed respectively Δi_{int} and Δa_{int} from target to by achieving by direct manoeuvring.

Direct orbital manoeuvring path

In addition to coasting relocation, it will be necessary two direct paths of manoeuvres. One for suit coasting drifting orbit from initial user satellite position,

$\Delta x_{initial} \rightarrow \Delta x_{int}$, and the last one from drifting orbit to the desired target $\Delta x_{int} \rightarrow \Delta x_t$. This one should be the most accurate as possible if we want to set the defined formation with precision.

In the first iteration, manoeuvres will be considered impulsive, which later should be converted to long low-thrust manoeuvres. To fulfil this requisite, a maximum ΔV will be imposed per manoeuvre. This value must be set according to manoeuvre duration and propulsion power unit, which never gets over one semi-period duration. Because of this, two manoeuvres will be performed per orbit during manoeuvring time.

To compute these manoeuvres, we first establish the mathematical foundation. Specifically, we turn to Gauss's variational equations for classical orbital elements (GVEs). An impulsive manoeuvre comprises three components: the radial, transverse, and normal components.

In impulsive manoeuvres, the GVEs establish a direct relationship between the orbital elements and the acceleration elements in the LVLH frame. To avoid multiple conflicts with the argument of latitude, equinoctial eccentricity will be used instead, as formulated in [5] (13).

$$\begin{aligned} \frac{da}{dt} &\approx 2a \frac{\gamma_T}{na} \\ \frac{du}{dt} &\approx n - 2 \frac{\gamma_R}{na} - \frac{\sin u \gamma_N}{\tan i na} \\ \frac{de_x}{dt} &\approx 2 \cos u \frac{\gamma_T}{na} + \sin u \frac{\gamma_R}{na} \\ \frac{de_y}{dt} &\approx 2 \sin u \frac{\gamma_T}{na} - \cos u \frac{\gamma_R}{na} \\ \frac{di}{dt} &\approx \cos u \frac{\gamma_N}{na} \\ \frac{d\Omega}{dt} &\approx \frac{\sin u \gamma_N}{\sin i na} \end{aligned} \quad (13)$$

Due to u and Ω will be corrected by coasting orbit drifting, these parameters and subsequently errors will

be ignored in manoeuvring direct paths. Taking increments of previous equations, where acceleration converts into single impulses $\Delta V = (\Delta V_r, \Delta V_t, \Delta V_n)$ and orbital parameters differences to corrected from initial orbit and coasting orbit, and from coasting orbit to target $\Delta a, \Delta e_x, \Delta e_y$, and Δi , it is possible to combine them in (14).

$$\begin{aligned} \Delta a &\approx 2a \frac{\Delta V_t}{na} \\ \Delta e_x &\approx 2 \cos u \frac{\Delta V_t}{na} + \sin u \frac{\Delta V_r}{na} \\ \Delta e_y &\approx 2 \sin u \frac{\Delta V_t}{na} - \cos u \frac{\Delta V_r}{na} \\ \Delta i &\approx \cos u \frac{\Delta V_n}{na} \end{aligned} \quad (14)$$

They allow us to compute analytically directly the total ΔV to perform by giving parameter variations to correct. This can be done by a pair-manoevre strategy, ΔV_1 and ΔV_2 setting a manoeuvre in a predefined u_0 , and opposite the other, in $u_0 + \pi$, Fig. 6.

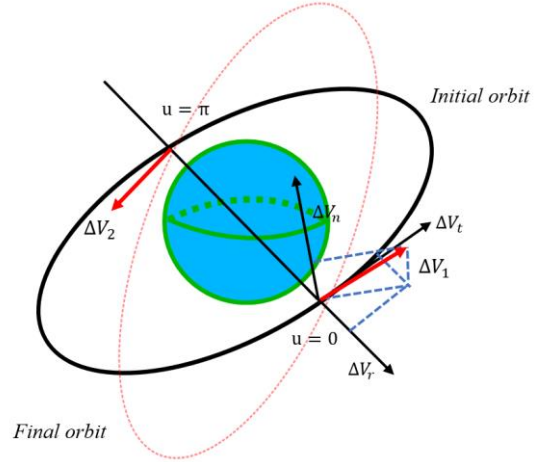


Fig. 6. Pair of direct manoeuvre schema

Applying this strategy, to achieve approximately the desired variation it is possible to reduce half part of the increment, $\Delta a/2$, $\Delta i/2$ and $\Delta e/2$ during the first manoeuvre and the remaining part during the second manoeuvre. This results in a sum of both terms in perigee and subtraction of the second term from the first in apogee. On the other hand, out-of-plane variations usually are highly expensive manoeuvres, so to increase the performance, the manoeuvre always will be done in the ascending/descending node, centering the impulses in the argument of latitude value of $u = 0$ for manoeuvre ΔV_1 and $u = \pi$ for manoeuvre ΔV_2 . With this approach, Δe_x will be corrected with tangential manoeuvres, and Δe_y with radial manoeuvres. Therefore, is possible to compute the total achieving variation of the parameters by combining (14) accurately in (15) for ΔV_1 and (16) for ΔV_2 .

$$\overline{\Delta V}_1(u=0) \begin{cases} \Delta V_{r1} = -\frac{na\Delta e_y}{2} \\ \Delta V_{t1} = \frac{n\Delta a}{4} + \frac{na\Delta e_x}{4} \\ \Delta V_{n1} = \frac{na\Delta i}{2} \end{cases} \quad (15)$$

$$\overline{\Delta V}_2(u=\pi) \begin{cases} \Delta V_{r2} = \frac{na\Delta e_y}{2} \\ \Delta V_{t2} = \frac{n\Delta a}{4} - \frac{na\Delta e_x}{4} \\ \Delta V_{n2} = -\frac{na\Delta i}{2} \end{cases} \quad (16)$$

Most of the cases de total ΔV_1 or ΔV_2 modulus surpasses the maximum ΔV_{max} allowed per manoeuvre (propulsion time after conversion to continuous manoeuvre). Therefore, the total ΔV should be reduced proportionally (17) as calculated in (15) and (16), and the variations proportions are conserved. The manoeuvre is considered as saturated.

If $\max(\|\Delta V_1\|, \|\Delta V_2\|) > \Delta V_{max}$ then

$$\begin{cases} \overline{\Delta V}_1 sat = \frac{\overline{\Delta V}_1}{\max(\|\Delta V_1\|, \|\Delta V_2\|)} \Delta V_{max} \\ \overline{\Delta V}_2 sat = \frac{\overline{\Delta V}_2}{\max(\|\Delta V_1\|, \|\Delta V_2\|)} \Delta V_{max} \end{cases} \quad (17)$$

According to this condition Δa , Δe_x , Δe_y , and Δi maybe will be lower as needed (18). So, to finally perform all parameters corrections proposed, a subsequence of pairs of manoeuvres will be performed, iteratively, until ΔV are not saturated. Therefore, a multi-pair manoeuvre path is created.

$$\begin{aligned} \Delta a_{sat} &= 2 \frac{(\Delta V_{t1} + \Delta V_{t2})}{n} \\ \Delta e_{x sat} &= 2 \frac{\Delta V_{t1} - \Delta V_{t2}}{na} \\ \Delta e_{y sat} &= -\frac{\Delta V_{r1} - \Delta V_{r2}}{na} \\ \Delta i_{sat} &= \frac{\Delta V_{n1} + \Delta V_{n2}}{na} \end{aligned} \quad (18)$$

Station Keeping optimization.

Evaluating the performance of the formation after algorithm development, an extra point arises, the possibility of optimizing the formation's station-keeping by slight modification in orbit target, to maximise the posterior time after relocation without Station-Keeping (SK) manoeuvring. This optimization leverages the drag-driven parabolic behaviour of the argument of latitude. Due to differences in atmospheric drag, when the follower semi-major axis decreases Δa_{atm} , the argument of latitude u drifts faster and exceeds the bounds of the leader-follower formation sooner, Fig 7.

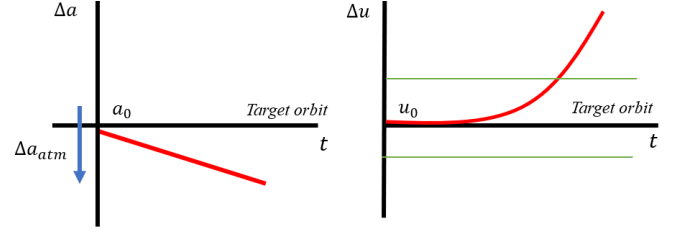


Fig. 7. Natural evolution of Δu due to drag differences without an optimized induced target.

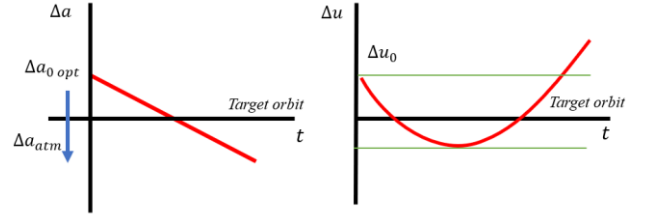


Fig. 8. Evolution of Δu due to drag differences with optimized $\Delta a_{0 opt}$ and Δu_0 over target.

Shifting our focus to the Δu evolution to minimize the increment along the time, Fig. 8, the equation for the secular linear drift of the argument of latitude caused by perturbations are previously expressed. We can assume in the first approximation that the perturbation of J_2 is negligible concerning the orbital revolution rate, conclude that the argument of latitude's evolution can be approximated as mean period $\dot{u}_{sec} = n$. Now that we have an expression for the argument of latitude's drift, the incremental variation of \dot{u} (19).

$$\Delta \dot{u} = \Delta n \quad (19)$$

Is possible to introduce incremental values by direct Taylor series expansion in mean motion $n^2 = \mu/a^3$, where only has a dependence. The drifting evolution difference of the argument of latitude is presented in (20).

$$\Delta \dot{u} = -\frac{3n}{2a} \Delta a(t) \quad (20)$$

Where $\Delta a(t)$ will be the evolution during the SK of the semi-major axis difference between real follower satellite orbit and target orbit, attached to leader satellite. Considering $\Delta a(t)$ independently from the rest of variables, $\Delta a(t) = \Delta a_0 + \Delta a(t)$, it is possible to integrate directly $\Delta \dot{u}$ (21), where $\Delta a(t)$ is the evolution of user satellite orbit due to drag differences.

$$\Delta u = -\frac{3n}{2a} \int_0^{t_f} [\Delta a_0 + \Delta a(t)] dt \quad (21)$$

$\Delta a(t)$ evolution is known after a first iteration, when a direct relocation to the target orbit is performed, i.e. $\Delta a_0 = 0$. Mostly of LEO cases, $\Delta a(t)$ tends to be lineal

due to the proportionality of ballistic coefficient differences. According to that, it is possible to make the hypothesis: the argument of latitude's evolution follows a drag-driven pattern, experiencing a parabolic behaviour. So, the Δa_0 could be different to null, being possible to maximize the time within formation boundaries. To achieve this, to condition can be established: the incremental value of u will be zero $\Delta u(t_f) = 0$ at final time. The second condition implies $\Delta u(t_f/2) = -\Delta u_0$, i.e. at half of maximum time, Δu will be opposed in the parabola. Substituting and re-arranging, we obtain the system to solve (22).

$$\begin{aligned} \Delta a_0 &= -\frac{1}{t_f} \int_0^{t_f} \Delta a(t) dt \\ \Delta u_0 &= \frac{3n}{2a} \left(\frac{t_f}{2} \Delta a_0 + \int_0^{t_f/2} \Delta a(t) dt \right) \end{aligned} \quad (22)$$

Setting $\Delta u_0 = \Delta u_{max}$ as maximum threshold value distance, the previous integrals could be calculated numerically, maximizing the time without SK, t_f . The result Δa_0 will be directly applied to the target orbit of the follower.

C. Algorithm implementation

Once the main formulation is proposed, a numerical algorithm is implemented to compute the formation.

The first step involves calculating the target orbit based on the leader references orbit. Subsequently, using the user-defined distance threshold, the program checks if the user's real position is aligned in the tube with the calculated target during the provided timespan. If the follower satellite is in the intended formation with the leader, the program ends successfully, providing the calculated target orbit file as output. Conversely, if the follower satellite gets out from the formation threshold at any moment, or it is located directly outside at first instance, the program starts a dedicated subroutine to compute the necessary SK/Injection.

For Injection/SK manoeuvre computation, an optimized multi-step iterative methodology is implemented. As explained before, the delta parameters between the starting user orbit and the target orbit $\Delta a, \Delta e_x, \Delta e_y$ and Δi will be corrected directly with equivalent low-impulsive manoeuvres. On the other hand, the parameters $\Delta \Omega$ and Δu will be corrected by coasting drifting orbit during the appropriate time. The total needed drift is obtained by using a coasting orbit defined by an Δa_{int} and Δi_{int} over a target orbit. Depending on these delta values, the orbital arc to follow and the number of manoeuvres will be different. As follows, the number of manoeuvres modifies the available total drift time.

To deal with the problem, it has been solved by fixing a

maximum time imposed by the user t_{max} and considering $\Delta \dot{u}_{int}$ and $\Delta \dot{\Omega}_{int}$ the unknowns to solve the problem. By using a direct Newton-Raphson methodology and dealing adequately with time, is possible to get appropriate coasting orbit drifting values with higher precision, Fig. 9. The ultimate objective is approaching all delta orbital parameters to null at the end of the relocation time $\Delta x(t_f) \rightarrow 0$.

During the previous algorithm, it is possible to distinguish two different manoeuvring arcs, where $\Delta a, \Delta e_x, \Delta e_y$ and Δi parameters are corrected directly. From initial position to the coasting orbit $\Delta x_{initial} \rightarrow \Delta x_{int}$, another from coasting to the final one $\Delta x_{int} \rightarrow \Delta x_{final}$. An iterative algorithm is used for both. By setting a multiple pair-manoevre path strategy, they will be performed in ascending/descending nodes, and $\Delta V_i = (\Delta V_r, \Delta V_t, \Delta V_n)$ could be directly calculated by the proposed formulation in (15) and (16). It is worth noting that the calculated ΔV_i may sometimes exceed the maximum ΔV_{max} allowed requirement (17). If this happens, the proportional low-impulsive is settled (17).

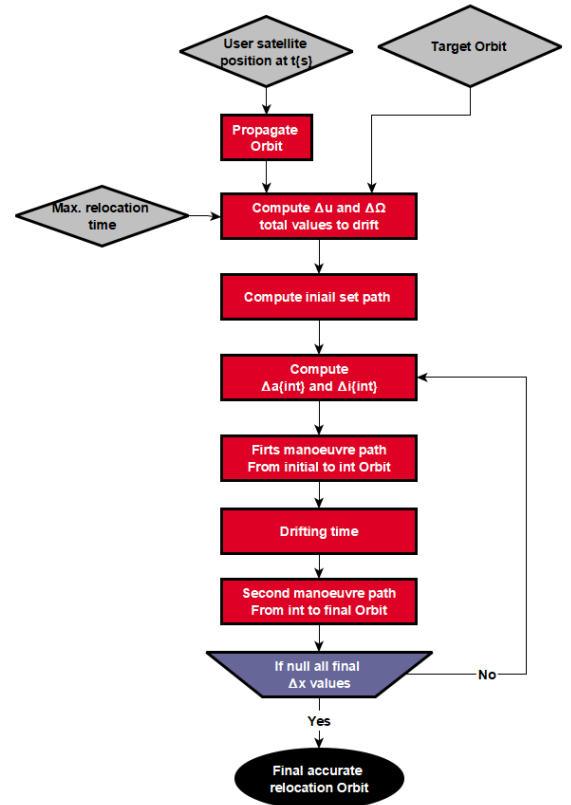


Fig. 9. Algorithm schema. Newton-Raphson to optimize drifting coasting orbit.

Later, the optimization SK evolution after target injection entails conducting another new iteration and execution of the modified Newton-Raphson method, by approaching the satellite orbit to a new slightly modified

target $\Delta a(t_f) \rightarrow \Delta a_{0\ opt}$ and $\Delta u(t_f) \rightarrow \Delta u_{0\ opt}$, Fig. 10. Joining all subsequent processes, the final algorithm is developed.

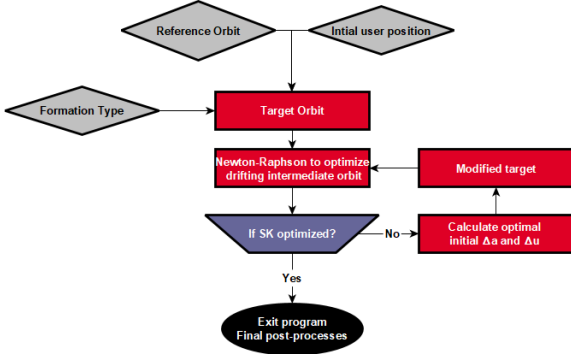


Fig. 10 Algorithm schema. Final SK optimization by target modification.

III. RESULTS

To validate the operability and prove the feasibility of our program, multiple analyses have been performed. First, pure leader-follower formation analysis was performed, by three different test cases in a pure leader-follower strategy: the injection into formation from a launcher error, an SK maintaining operation. Later, other results will be presented about the rest of the formations.

As previously mentioned, our scenario involves two satellites: the leader of the formation, the reference orbit, and its follower. To ensure a comprehensive evaluation of outcomes, it is essential to consider the different physical characteristics of these satellites.

The main perturbing forces considered by the program for propagation, which mainly acts on a spacecraft in a sun-synchronous orbit are 32 Degrees and Orders of geopotential terms, aerodynamic drag ($F_{10.7} = 127.4$ for 50 percentile), Gravitational effects of the Moon and the Sun, solar radiation pressure, solid tides and ocean tides.

The ballistic coefficient C_b is important to understand the interaction between both satellites. The higher the C_b , the lower the atmospheric drag the satellite would experience. Comparing both satellites, the Follower satellite will present a higher drag force concerning Leader one. Consequently, this deviation will lead to a more pronounced deceleration of the Follower, prompting a reduction in the semi-major axis and subsequently its orbital period. This effect, compounded by the perturbations that affect the satellite in LEO, will contribute to a modification in the inter-satellite distance: approaching the two satellites if the Follower

is behind the Leader, and vice-versa, moving away if the follower is ahead.

To analyse the following formations, our focus is on analysing how is the evolution in radial (R), along-track (S), and cross-track (W) coordinates of the Synchronised Satellite Coordinate System. The origin of this reference system is the reference orbit of the leader.

A. Pure Leader-Follower operational tests

Using the initial conditions explained before, two scenarios are analysed for the Leader-Follower strategy:

- Formation Injection.
- Formation Station Keeping.

Each one is explained in the following sections.

Leader-Follower Formation injection

The initial scenario involves establishing a simple leader-follower formation with an inter-satellite distance of 100 km in the along-track direction, following a steady trajectory set by the leader satellite. A 40-day maximum time was set to perform the complete relocation. A maximum of 1 m/s ΔV per manoeuvre was used.

Table 1. Initial position in osculating elements after user satellite launcher deployment

	Target	Follower
Epoch	2023/01/01-00:00:00.000	
a (km)	7006.8609	7003.8609
e	0.001185	0.0013
i (deg)	97.863	97.83
Ω (deg)	186.364	186.42
ω (deg)	90.257	98.257
θ (deg)	150.870	269.870

Table 2. Final position in osculating elements after user satellite launcher deployment

	Target	Follower
Epoch	2023/02/10-00:00:00.000	
a (km)	6997.63265	6997.63265
e	0.00025	0.00025
i (deg)	0.00154	0.00154
Ω (deg)	97.79200	97.79200
ω (deg)	225.77262	225.77262
θ (deg)	182.41651	182.41651

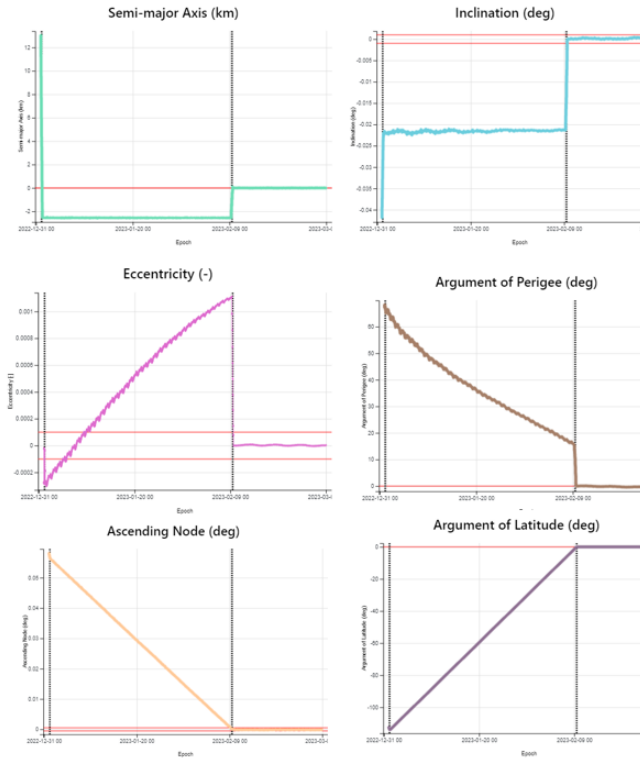


Fig. 11 Delta Keplerian mean elements between user satellite and settled target in a Leader-Follower

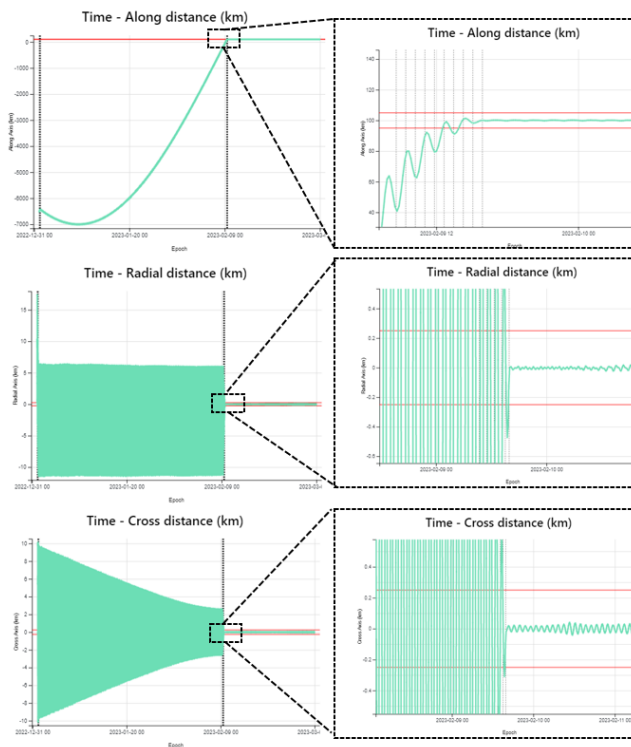


Fig. 12 RTN plots centered on leader satellite during user satellite injection.

With input data settled in Table 1, the test was executed. First, the program calculates the target orbit from the Leader satellite. Later, it iterates Δu and $\Delta \Omega$, thanks to a coasting transference orbit, converging in only six iterations, as seen clearly in Δ element, Fig. 11. The program launches the successive manoeuvre strategy to reach with higher precision the searched target. The satellite only needs to perform 20 manoeuvres, with a total $\Delta V = 14.452$ m/s. Finally, the follower satellite orbit with manoeuvres is propagated and the results are generated, Table 2, showing the follower satellite accurately injected in a 100 km inter-distance position from the leader satellite as per Fig 12.

Leader-Follower Formation SK

Once the formation is established, it is needed to perform station-keeping manoeuvres from time to time. The algorithm of SK formation works similarly to injection one, but with an extra first step: It identifies when the follower satellite orbit goes outside the threshold “tube” around the target orbit that it is driven by the leader satellite. The initial condition of this test is the output of the previous injection test. The thresholds were set to 5 km in along-track, and 0.25 km maximum in radial and cross distances.

At the initial moment, both satellites are in formation, where the Follower satellite is placed ahead of the Leader. To understand the results, as explained before, due to the differences in C_b , the Follower satellite experiences more drag than the Leader satellite. With a decrease of the semi-major axis, the Follower satellite started to get away from the Leader. At some point, the inter-satellite distance reaches the maximum allowed threshold (5km), so will be necessary to perform a SK manoeuvre, Fig. 13. For additional SK optimization, the target will not be the centre of the tube. The optimal point presented, Table 3, allows the satellite to maximize the time inside the SK window. The algorithm only needs 4 manoeuvres with a total $\Delta V = 0.1664$ m/s.

Table 3. Target relocation modification to optimize SK.

Target Modification	
Δa_0 (m)	10.79473
Δu_0 (deg)	0.01643

The results, Fig. 14, clearly demonstrate the successful SK cycle. More importantly, it illustrates how the follower satellite takes advantage of the difference in the natural drag, for inducing a parabolic evolution of the Argument of Latitude. The manoeuvre maximizes the time within the SK window without requiring extra manoeuvres. This approach significantly aids in minimising fuel consumption.

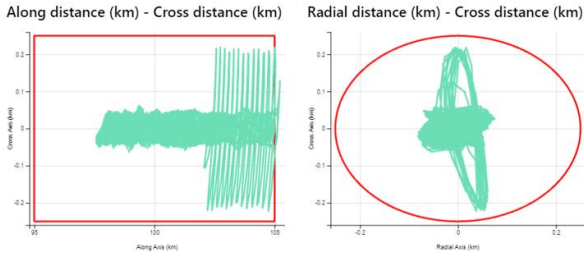


Fig. 13 Composed RTN plot, where SK is performing showing the evolution between components.

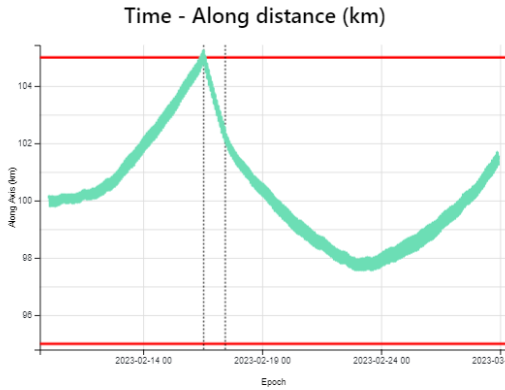


Fig. 14 Along distance – Time plot, where SK is performing centred on 100 km with 5 km threshold.

B. Other Formation strategies. Results.

For the rest of the formations, the same properties and initial conditions as explained in Leader-Follower are assumed. First, an initial relocation for formation injection is performed. Later, multiple SK sequences can be done. First, could be similar to the pure Leader-Follower formation, but with different manoeuvring results in order to inject according to the selected type and orbital parameters. But SK results are especially interesting because they show the formation behaviour and the “dance” between both satellites.

Cartwheel Formation SK

To establish a cartwheel formation, during the injection, a modification of the direction of the eccentricity vector was applied, a oppose perigee $\delta\omega=180^\circ$ is incorporated. After injection, the formation was achieved.

The direct results show an interesting orbital trajectory from the Follower satellite over the leader reference satellite, Fig. 15. The cartwheel formation’s response to orbit perturbations presents consistent J_2 secular effects across both satellites. This common influence involves the precession of ascending nodes, affecting each satellite uniformly. That throws an interesting cylindrical pattern.

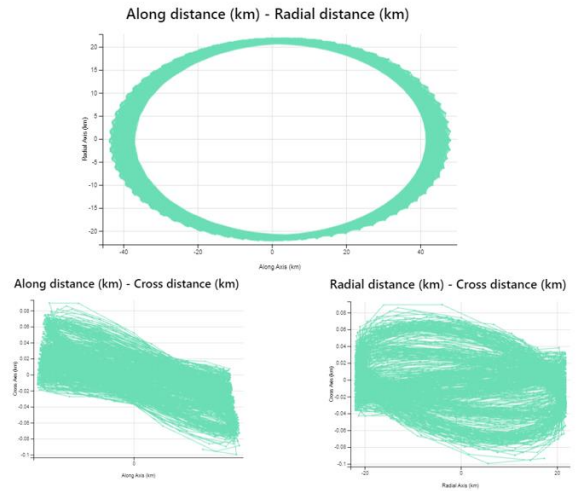


Fig. 15 Composed RTN plots, where SK is performing showing the evolution in Cartwheel strategy.

However, after some days, the inter-satellite distance starts to oscillate and must be corrected. That happens because of incredible variations in the argument of latitude behaviour (out of frozen orbit) and drag differences. If the trajectory is not corrected, the paths of the satellites could intersect, raising the risk of potential collisions.

Pendulum Formation SK

The pendulum formation is generated by a difference in Ω to achieve a non-zero cross-track component as well as a difference in mean anomaly to avoid the risk of collision between the two satellites. For this test case, the variations applied are $\delta u=-0.5^\circ$ and $\delta\Omega=1^\circ$.

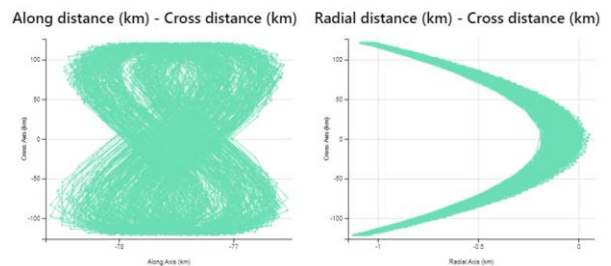


Fig. 16 Composed RTN plots, where SK is performing showing the evolution in Pendulum strategy.

The orbital simulated result between the two satellites, Fig. 16, exhibits a pendulum-like behaviour in the radial-cross plot comparative, while an eight-figure trajectory is drawn in the along-cross plot. Notably, the inter-satellite distance experiences an initial decrease in the first days followed by an increasing trend. Multiple SK manoeuvres must be performed to keep the formation.

Helix Formation SK

The Helix formation strategy resembles a safety ellipse movement elaborated by two synchronized satellites. To effectively execute this strategy, we need precise adjustments between the follower and leader, with a $\delta\Omega=0.5^\circ$ shift., a opposite perigee $\delta\omega=180^\circ$, and $\delta u=-0.5^\circ$ in the argument of latitude to avoid collision risk.

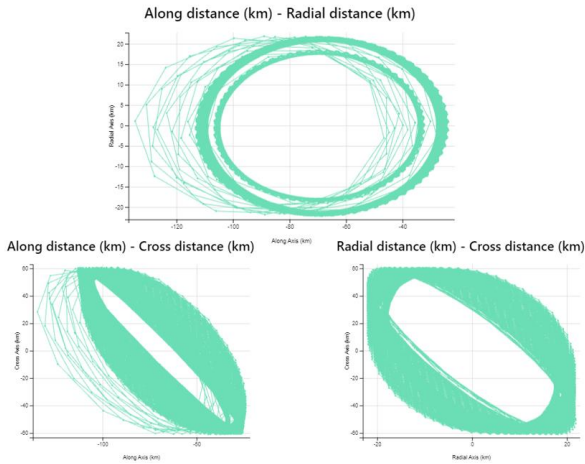


Fig. 17 Composed RTN plots, where SK is performing showing the evolution in Helix strategy.

The evolution of this formation closely parallels the pendulum mixed with cartwheel formation. The plot throws a notable distinction in the radial-along track plot, Fig. 17. The time evolution shows an inter-satellite oscillation-like cartwheel formation in different “radial” circumferences. Also, in the along-cross plot, an “eight-figure” trajectory, is reminiscent of the helix strategy. In radial-cross, an inherited “pendulum” is visible from the last proposed strategy.

IV. CONCLUSIONS

A new operational algorithm has been successfully implemented and integrated inside GMV’s Flight Dynamics product *Focussuite*, called FAMA. GMV’s flight-proven solution is now able to compute the necessary manoeuvres to acquire and maintain different formation flying strategies such as pure leader-follower, cartwheel, pendulum, and helix. Each of them with successful results and for different applications. These strategies are useful for several future missions and increase the flexibility of *Focussuite* to be able to operate any kind of mission.

V. REFERENCES

- [1] D. A. Vallado, “Fundamentals of astrodynamics and applications,” *Springer Science & Business Media*, 2001, vol. 12.
- [2] Gim J. Der and Roy Danchick, “Conversion of Osculating Orbital Elements to Mean Orbital Elements” *TRW 1996*.
- [3] Hanspeter Schaub, “Spacecraft relative orbit geometry description through orbit element differences” *ORION International Technologies, Albuquerque, NM 87106, 2002*
- [4] Jonathan W. Wright, “Minimizing secular j_2 perturbation effects on satellite formations” *Wright-Patterson Air Force Base, Ohio, Germany 2008*.
- [5] Mohamed Khalil Ben Larbi, Enrico Stol, “Spacecraft formation control using analytical integration of Gauss variational equations” *Institute of Space Systems, Germany 2018*.
- [6] Arianespace, “*Small Spacecraft Mission Service VEGA-C. User’s Manual*”, Boulevard de l’Europe. Sept. 2020